Asghar Zamani*, Ahmad Poursattar Marjani* and Mojtaba Abedi Mehmandar

Synthesis of high surface area magnesia by using walnut shell as a template

https://doi.org/10.1515/gps-2018-0066
Received March 16, 2018; accepted June 13, 2018; previously published online July 20, 2018

Abstract: In the present study, high surface area amorphous magnesia was synthesized using walnut shell as a template. This green, simple and useful synthetic protocol was based on the precipitation of magnesium nitrate on biomass in an aqueous phase, followed by calcination. Materials were characterized using X-ray diffraction, scanning electron microscopy (SEM) and N_2 adsorption/desorption porosimetry, and the results exhibited high surface area for magnesium oxide. Furthermore, the pore size and surface area of these mesoporous materials can be adjusted by varying the biomass/magnesium nitrate ratio. In addition, magnesium oxide was studied as the support of palladium nanoparticles for the aerobic oxidation of alcohols. We have found out that the resulting Pd-loaded material acts as an effective catalytic system for the aerobic oxidation of benzylic and aliphatic alcohols. The catalyst can be recovered and reused three times without loss of activity. Also, to test the catalytic activity of magnesium oxides as a solid catalyst, we selected Meerwein-Ponndorf-Verley reduction of cyclohexanone with 2-propanol over different magnesium oxides.

Keywords: agricultural waste biomass; alcohols; catalysis; green chemistry; nanostructures; surface area; textural properties.

1 Introduction

Material chemists are interested in magnesium oxide or magnesia (MgO) because of its outstanding properties, such as lowest solubility among the alkaline earth oxides, easy obtainability and cheapness, as well as its textural properties, such as high surface area. Nowadays, magnesia nanomaterials are widely employed in various areas, such as paint, adsorption, superconductivity, catalysis and toxic waste elimination [1–3].

Several preparative procedures for the synthesis of high surface area magnesia have been reported. While one of the simplest methods to prepare nanoporous MgO with relatively low surface area (97–161 m^2g^{-1}) is through hydrothermal treatment of commercial bulk MgO crystals in water [4] or magnesium salts in mixed solvents of ethylenediamine and water [5] followed by calcination, some chemists have synthesized magnesium oxide with higher surface area (72–361.5 m^2g^{-1}) using co-precipitation method by magnesium nitrate and ammonia or urea [6–8]. Another strategy focuses on the synthesis of magnesium bicarbonate $Mg(HCO_3)_2$ by bubbling CO_2 into aqueous suspension of commercial magnesium oxide. By calcination of magnesium carbonate prepared from $Mg(HCO_3)_2$, porous MgO was synthesized [9, 10]. Magnesium oxide nanoparticles can be synthesized by hydrolysis of magnesium alkoxide $Mg(OCH_3)_2$ in a toluene-CH_3OH solvent [11, 12]. Calcination of the synthesized gel resulted in the formation of magnesia with surface area of 201–503 m^2g^{-1}. Evaporation and oxidation of Mg pieces at 913 K and in high vacuum in quartz glass tube resulted in MgO nanocubes with particle size distribution in the range of 10–1000 nm and surface area up to 300 m^2g^{-1} [13].

In separate studies, Li et al. and Purwajanti et al. described mesoporous magnesia preparation using hard-templating method by mesoporous carbon prepared by pyrolization of resorcinol/formaldehyde polymer as a template [14, 15]. Nanoporous MgO was also obtained by the mesoporous carbon hard-templating method, and the corresponding surface area can reach up to 175 m^2g^{-1}.

Three-dimensionally ordered macroporous magnesium oxide has been prepared by using triblock copolymer $EO_{106}PO_{70}EO_{106}$ (Pluronic F127) as a surfactant and monodispersive polymethyl methacrylate (PMMA) microspheres as a hard template, which was removed by high-temperature calcination [16]. The magnesia samples prepared with this method possessed high surface areas (125–243 m^2g^{-1}). Nanoporous magnesium oxide with maximum BET surface area of 66.25 m^2g^{-1} was prepared by simple hydrothermal method using urea as precipitating agent in the presence of polyethylene glycol (PEG400) as template [17]. Yang et al. reported the synthesis of

---

***Corresponding authors: Asghar Zamani,** Nanotechnology Research Center, Urmia University, Urmia 57154, Urmia, Iran, e-mail: a.zamani@urmia.ac.ir; and **Ahmad Poursattar Marjani,** Department of Organic Chemistry, Faculty of Chemistry, Urmia University, Urmia, Iran, e-mail: a.poursattar@urmia.ac.ir
Mojtaba Abedi Mehmandar: Nanotechnology Research Center, Urmia University, Urmia 57154, Urmia, Iran

flowerlike magnesia with high surface area of 343 m^2g^{-1} by solvothermal route using ammonium hydroxide as precipitating agent and ethylene glycol as solvent in the presence of povidone with an average molecular weight of 40,000 [18].

Although various methods for the synthesis of high surface area magnesia with controllable textural properties have been reported, these methods usually use non-aqueous solvent (e.g. ethylene glycol), precipitating agents (e.g. ammonia and urea) and synthetic template (e.g. polymers and mesoporous carbon). These conditions encounter environmental and economical challenges in large-scale application. For these reasons, synthesis of mesoporous MgO in aqueous phase without any unsafe chemicals has attracted intensive attention. From a green chemistry point of view, agricultural waste biomass can also be recognized as valuable resource in the chemical synthesis and production of fuels [19]. Attention in biomass transformation to fuel and other chemical compounds has dramatically increased in the last decade within academic and industrial fields, with the support of NGOs and governments, because of their bio-based and renewable chemicals, which have many benefits, such as reduction of greenhouse gases and reduction of chemical contamination [20–22].

Herein, magnesia was prepared by impregnation and hydrothermal process in the presence of walnut shell as a template and magnesium nitrate as a magnesium source, and its catalytic activity in the aerobic oxidation of alcohols and Meerwein-Ponndorf-Verley (MPV) reduction was also studied.

2 Materials and methods

2.1 Materials

Magnesium nitrate hexahydrate ($Mg(NO_3)_2 \cdot 6H_2O$), palladium(II) chloride, toluene and other chemicals were purchased from Merck (Merck KGaA, Darmstadt, Germany) and used without further purification. The walnut shell from a local walnut tree in Urmia, Iran, was crushed using with a high-speed rotary cutting mill and screened to collect the particles with a size smaller than 0.45 mm. All chemicals were used without further purification.

2.2 Magnesia preparation

Magnesia was prepared by magnesium nitrate hexahydrate in the presence of 10-g walnut shell powder using various different magnesium/biomass ratios: 4:96, 8:92 and 12:88 in 100 ml of deionized water (Millipore, Milli-Q grade) at room temperature. After 5-h stirring, water from resulting mixture was evaporated by rotary evaporator under low pressure to give a brown solid. This solid was subsequently calcined in an electrical furnace in air (4:96, MgO-1; 8:92, MgO-2; and 12:88, MgO-3) at 500°C for 4 h (at a heating rate of 10°C/min). Resulting solids (materials A) were stirred in 50 ml of deionized water for 5 h under refluxing conditions followed by drying and calcination at 500°C for 4 h to give white powder (materials B: re-MgO-1, re-MgO-2 and re-MgO-3). For comparison, reference samples MgO-0 and re-MgO-0 were produced by the same way but without the use of biomass.

2.3 Catalyst preparation

MgO-supported palladium nanoparticle (PdNP) catalyst was synthesized by impregnation method. Na_2PdCl_4 was prepared from $PdCl_2$ (0.04 g) and NaCl (0.027 g) in water (50 ml). Two grams of re-MgO-2 was mixed with the abovementioned Na_2PdCl_4 solution at room temperature for 12 h. Water from the resulting mixture was evaporated by rotary evaporator under low pressure. The resulting solid was subsequently calcined at 250°C in air for 2 h. Finally, this solid was refluxed in ethanol for 1 h, followed by filtration and drying in 80°C (PdNP@re-MgO-2). The loading of palladium was determined using atomic absorption spectroscopy and showed loading at 0.1 $mmolg^{-1}$.

2.4 Characterization

The textural parameters were analyzed by N_2 adsorption experiments using Bel Japan Belsorp-mini II, analyzer at 77 K. Before measurement, the materials were degassed at 473 K for 5 h. The total surface areas were calculated with the multipoint Brunauer-Emmett-Teller (BET) method. X-ray diffraction patterns (XRD) of the obtained materials were recorded at room temperature on Shimadzu XRD-6000 diffractometer (Kyoto, Japan) with Cu-Kα radiation. The morphology of materials was observed by TSCAN VEGA II XMU SEM Instrument (Czech Republic).

2.5 Oxidation reaction

Typically, the aerobic oxidation of alcohols was carried out in 25-ml flask equipped with a reflux condenser in undried toluene as solvent. A mixture of the alcohol (1 mmol) and PdNP@re-MgO-2 in undried toluene (5 ml) was prepared in a two-necked flask. This mixture was stirred at 80°C under the atmospheric pressure of O_2 or air (balloon filled). The oxidation reaction progression was checked by silica gel TLC. At the end of the reaction, the catalyst was filtered, and gas chromatograph (Shimadzu, GC-2010) showed product yields.

2.6 MPV reduction

Typically, to a solution of cyclohexanone (3 mmol), in 5 ml of 2-propanol was added 0.5 g of magnesium oxide. The reaction mixture was heated to reflux temperature under magnetic stirring. Product yield was analyzed by gas chromatography (Shimadzu, GC-2010).

3 Results and discussion

In a typical experiment, walnut shell powder was dispersed into magnesium nitrate solution in deionized water. After stirring followed by evaporation of water, the solid obtained was transferred to a furnace and heated at 500°C for 5 h. XRD pattern of the prepared products (Figure 1) showed that magnesium nitrate precursor transforms MgO (JCPDS 75-0447) crystalline phase. N_2 adsorption/desorption isotherms for magnesium oxide samples (materials A) studied are shown in Figure 2. Textural parameters of these materials are also indicated in Table 1, entries 1–4.

As seen in Figure 2, according to the IUPAC classification [23], MgO-1 and MgO-2 exhibited type II isotherm and H3-shaped hysteresis loop in the relative pressure ($p/p0$) range of 0.8–1.0, which are characteristic properties of a mesoporous material with slit-shaped pores. Materials A has BET surface area and pore volume up to 79 m^2/g and 0.26 cm^3/g (MgO-2, Table 1, entry 3). Magnesium oxide prepared in the absence of walnut shell (MgO-0) has the lowest surface area and pore volume (44 m^2/g, 0.11 cm^3/g), which indicated that the presence of walnut shell is critical for the synthesis of mesoporous alumina (Table 1, entry 1). Figure 3A–D shows the BJH pore-size distribution of materials A. Most pore diameters in MgO-1 and MgO-2 samples are in the ranges of 4–14 nm and 4–12 nm, respectively (Figure 3B and C). From Figure 3A and D, one can observe that the MgO-0 and MgO-3 samples exhibited relatively broader pore-size distribution.

Figures 4 and 5 show the XRD pattern and N_2 sorption isotherms, respectively, for synthesized materials B by hydrothermal treatment of materials A under reflux conditions, followed by calcination in air. Surprisingly, the specific surface area of re-MgO-1 and re-MgO-2 samples

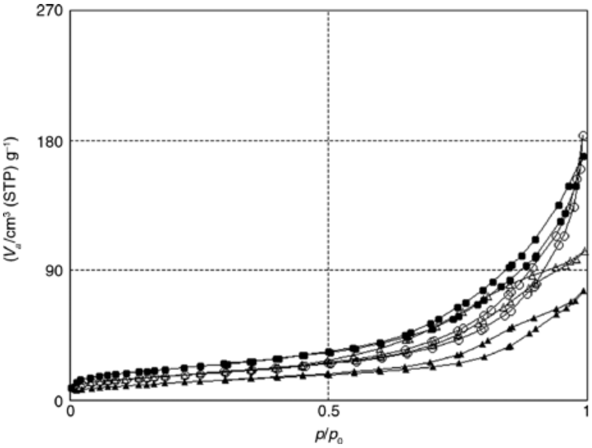

Figure 2: N_2 adsorptione/desorption isotherms of materials A.

Table 1: Textural properties of magnesia samples.

Entry	Sample	S_{BET} (m²/g)	V_{BJH} (cm³/g)	D_{BJH} (nm)
1	MgO-0	44	0.11	2.6
2	MgO-1	62	0.27	7.2
3	MgO-2	79	0.26	7.2
4	MgO-3	63	0.15	7.2
5	re-MgO-0	78	0.53	13.9
6	re-MgO-1	195	0.70	10.6
7	re-MgO-2	212	0.62	10.6
8	re-MgO-3	95	0.61	10.6

D_{BJH}, BJH average pore diameter; S_{BET}, BET surface area; V_{BJH}, BJH total pore volume.

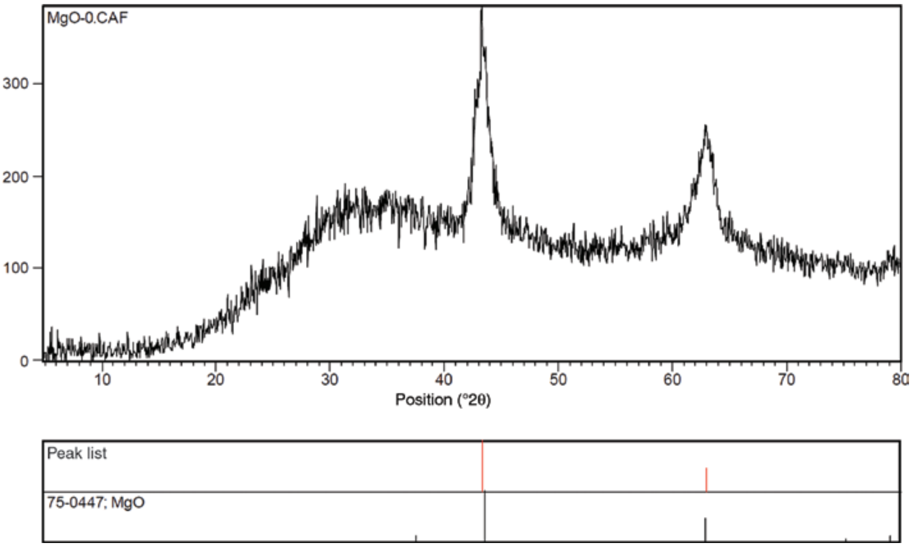

Figure 1: XRD patterns of MgO-2.

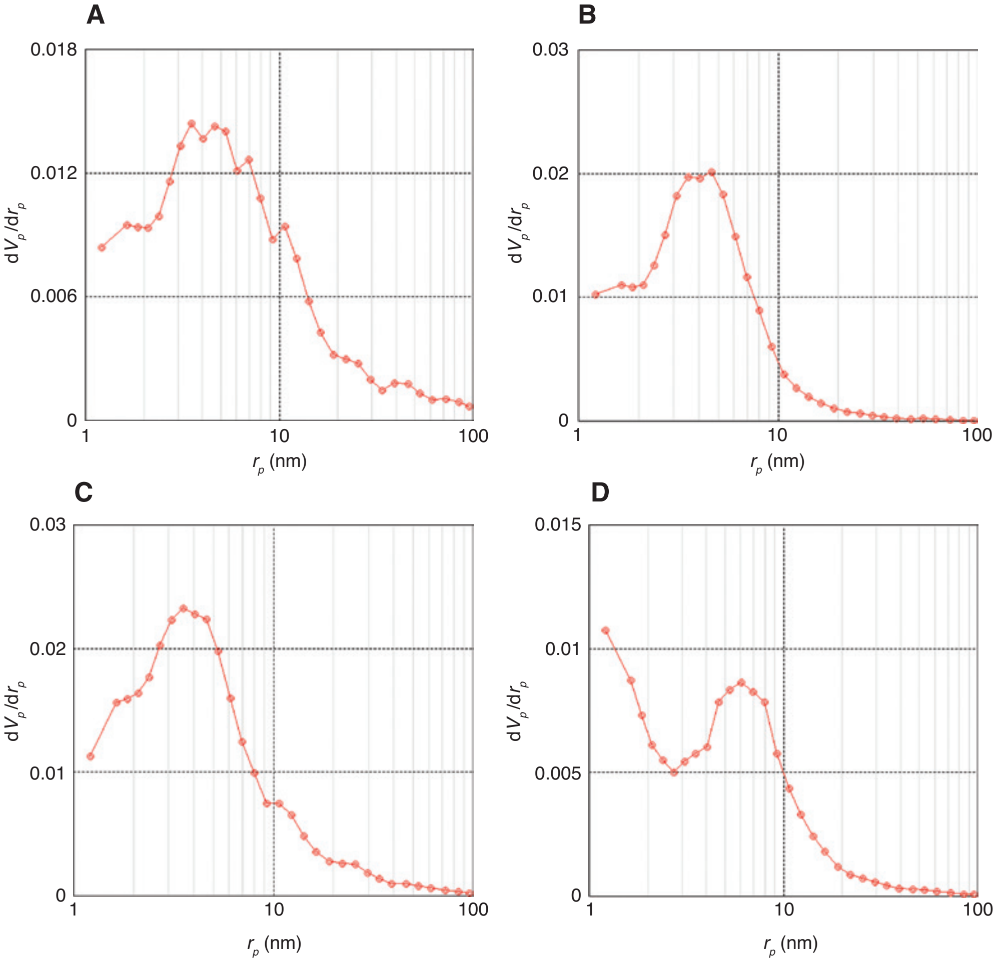

Figure 3: Pore-size distribution of materials A: (A) MgO-0, (B) MgO-1, (C) MgO-2, (D) MgO-3.

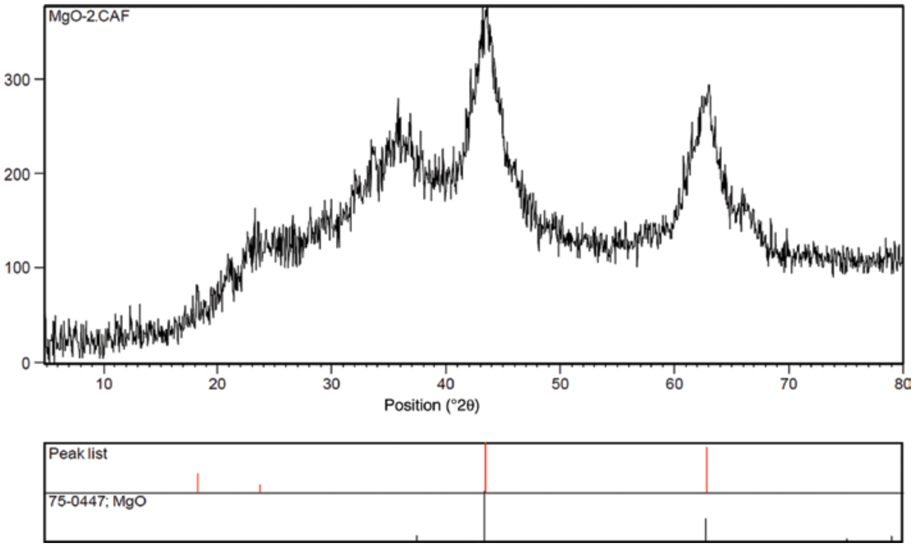

Figure 4: XRD patterns of re-MgO-2.

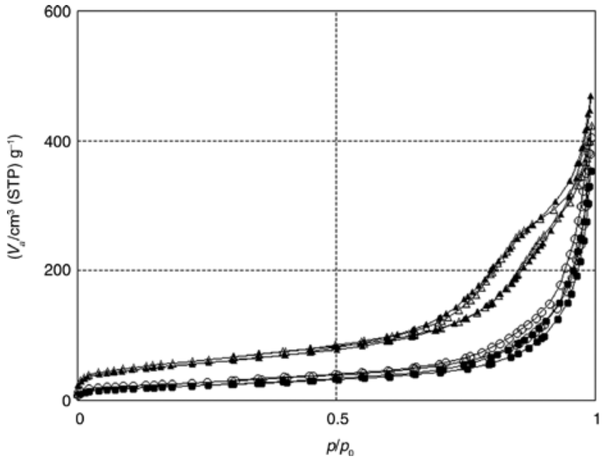

Figure 5: N_2 adsorptione/desorption isotherms of materials B.

increases from the range of 62 and 79 m²/g in MgO-1 and MgO-2 to 195 and 212 m²/g, respectively (Table 1, entries 6 and 7). Also similar behavior is found in re-MgO-0 and re-MgO-3. As seen in Figure 5, re-MgO-1 and re-MgO-2 exhibited type IV isotherm and the hysteresis loop can be classified as an intermediate between H1 and H3 types. However, N_2 adsorption/desorption isotherm measured for re-MgO-0 and re-MgO-3 is distinctive, being a type II isotherm, which is generally observed for macroporous materials (Figure 5). Figure 6A–D shows the BJH pore-size distribution of materials B. Most pore diameters in MgO-1 and MgO-2 samples are between 3 and 18 nm (Figure 6B and C). From Figure 6A and D, it can be detected that the MgO-0 and MgO-3 samples exhibited relatively broader pore-size distribution. SEM images of MgO-2 and re-MgO-2 reveal the nonrigid aggregates of plate-like particles forming slit-shaped pores (Figure 7).

A mechanism for the synthesis of the high porous magnesia can be suggested by which magnesium cations were dispersed on lignocellulosic biomass via coordination with their hydroxyl groups. Therefore, lignocellulosic component acts as a template for the magnesia precursors.

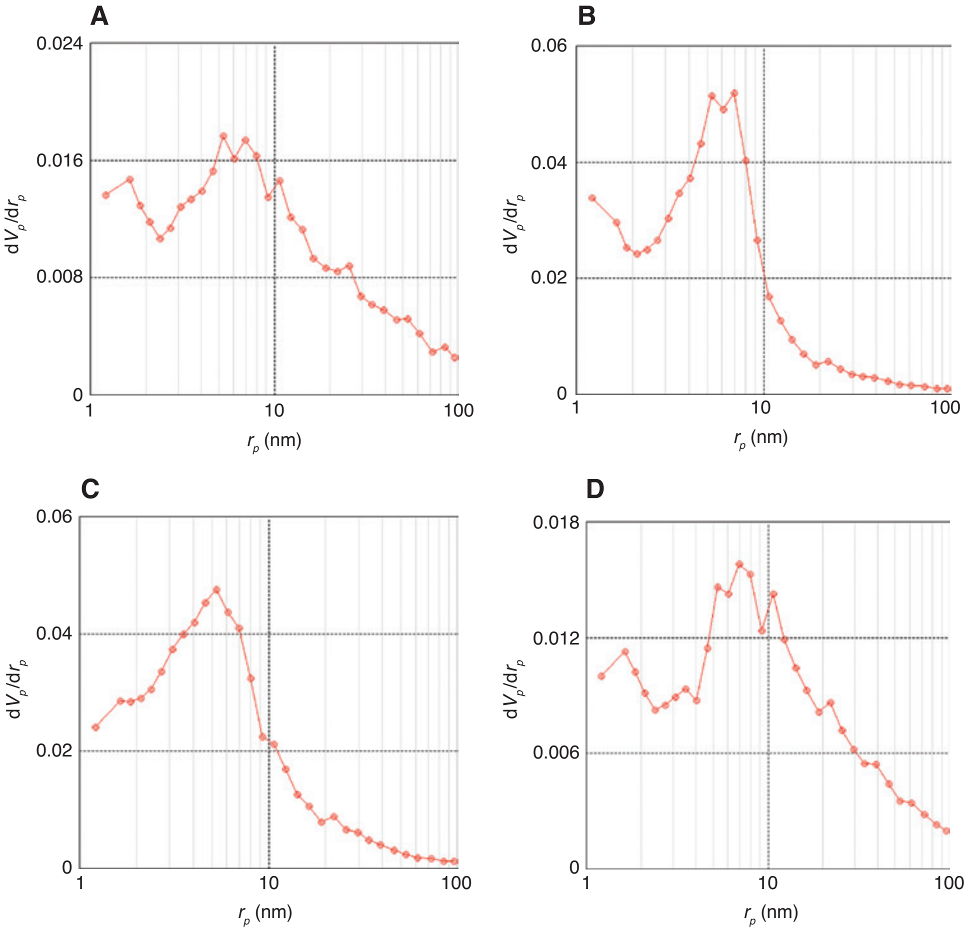

Figure 6: Pore size distribution of materials B: (A) re-MgO-0, (B) re-MgO-1, (C) re-MgO-2, (D) re-MgO-3.

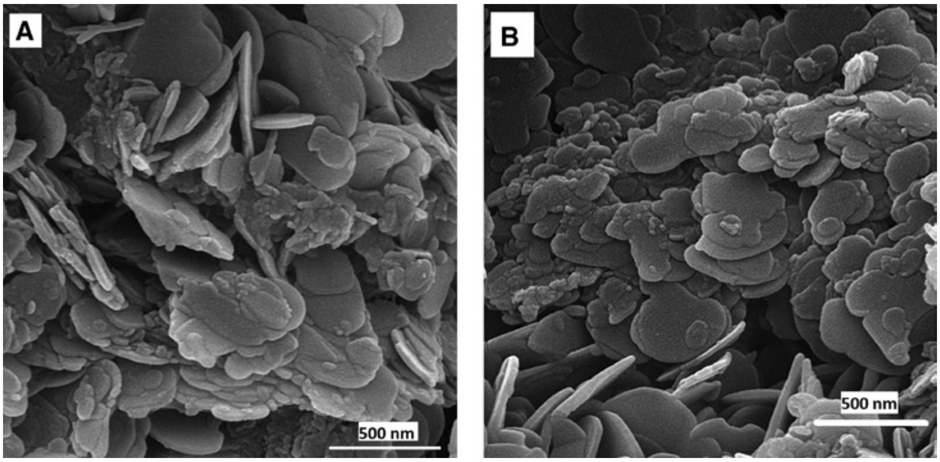

Figure 7: SEM of (A) MgO-2 and (B) re-MgO-2.

After dispersion of the Mg(II) on the template and increasing the temperature, the template was removed by transformation of CO, CO_2 and H_2O. Simultaneously with gas release from the template, magnesia is formed due to temperature increase. Magnesia should be highly porous due to two reasons, including (1) use of the template and (2) release of gases, which increases porosity.

Magnesia with the highest surface area, re-MgO-2, prepared by the walnut shell-templating technique was tested as catalyst support in the palladium nanoparticle (PdNP@re-MgO-2) aerobic oxidation of benzylic and aliphatic alcohols. TEM image of PdNP@re-MgO-2 in Figure 8 demonstrates that most sizes of Pd nanoparticles are between 8 and 17 nm. Table 2 demonstrates the catalytic oxidation reaction results of PdNP@re-MgO-2. Thus, benzyl alcohol was oxidized in the presence of PdNP@re-MgO-2 (0.25 mol%) in toluene at 80°C for 2 h (Table 2, entry 1) without the use of exogenous base or hydrogen acceptor additives and without additional purification and drying of solvent. Also, air has been used instead of molecular oxygen without any significant reduction in activity. After filtration of the reaction mixture, the catalyst was washed twice with CH_2Cl_2 and recycled. PdNP@re-MgO-2 also efficiently catalyzes the aerobic oxidation of 1-phenyl ethanol, 1-octanol and 2-octanol (Table 2, entries 5–7). This solid catalyst has been recovered and reused up to three times without significant loss of its activity (Table 2, entries 2–4).

Table 2: PdNP@re-MgO-2 catalyzed aerobic oxidation of alcohols.[a]

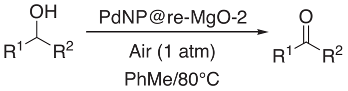

Entry	R[1]	R[2]	Cat. (mol%)	Time (h)	Yield (%)[b]
1	Ph	H	0.25	2	97
2	Ph	H	0.25	2	90[c]
3	Ph	H	0.25	2	91[d]
4	Ph	H	0.25	2	85[e]
5	Ph	Me	0.25	3	88
6	n-C_6H_{13}	Me	0.5	3	90
7	n-C_8H_{17}	H	0.5	3	87

[a] Reaction conditions: alcohol (1 mmol), PdNP@re-MgO-2, Toluene (5 ml) stirred under air at 80°C for the appropriate time.
[b] GC yield.
[c] First reuse.
[d] Second reuse.
[e] Third reuse.

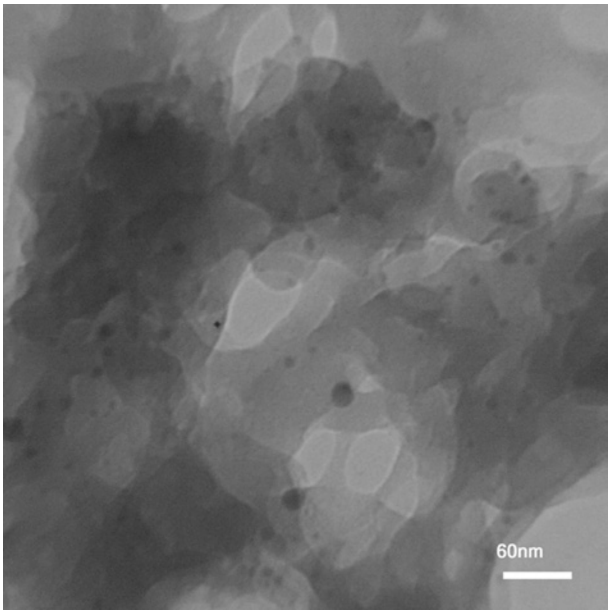

Figure 8: TEM of PdNP@re-MgO-2.

In order to illustrate the merit of our system for the aerobic oxidation of alcohols, we have shown the benefits

Table 3: Comparison of magnesia supported palladium nanoparticle catalysts for the aerobic oxidation of 1-octanol.

Entry	Magnesia (Pd mol%)	Solvent/Temp. (°C)	Time (h)	Yield (%)	Ref.
1	From calcination of magnesium nitrate, SA: 39 m^2g^{-1} (1)	$PhCF_3$/80	20	20[a]	[24]
2	Nanocrystalline magnesia, commercial, SA: 590 m^2g^{-1} (0.14)	PhMe/r.t.	20	68[b]	[25]
3	Our protocol (0.5)	PhMe/80	3	87[a]	

[a]Without exogenous base.
[b]With 1.2 equivalent K_2CO_3.

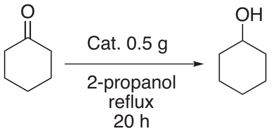

Cat.	Yield (%)
re-MgO-0	43
re-MgO-1	88
re-MgO-2	85
re-MgO-3	52

Scheme 1: Effect of surface area in MgO-catalyzed MPV reaction.

of present technique by comparing our outcomes with those previously stated in the literature for the magnesia-supported palladium nanoparticle catalyzed aerobic oxidation of 1-octanol. Based on previous reports (Table 3), this is one of the efficient catalytic systems in the aerobic oxidation of alcohols at the least time possible and without the presence of any added base in good yields (Table 3, entry 3). The yield of aerobic oxidation of 1-octanol catalyzed by PdNPs supported on MgO from calcination of magnesium nitrate is very low in an expansive solvent after 20 h (Table 3, entry 1). On the other hand, PdNPs supported on nanocrystalline magnesia afforded moderate yield at this time in the presence of an exogenous base.

To test the catalytic activity of magnesium oxides as a solid catalyst, we selected MPV reduction of cyclohexanone with 2-propanol over different magnesium oxides. This catalyst was found to be effective for this MPV reaction, and recovering and reusing the catalyst happened to be easy. We have investigated the effect of surface area of MgO in this reaction (Scheme 1). It is of interest that different surface areas of MgO exhibit different catalytic activities. re-MgO-1 and re-MgO-2 with the highest surface area NPs showed maximum activity.

4 Conclusion

In summary, a green, simple and useful synthetic protocol to produce high surface area mesoporous amorphous magnesia using walnut shell as a template in aqueous phase was presented above. Most importantly, the textural properties of materials were simply characterized in our studies using N_2 adsorption/desorption porosimetry. SEM analysis shows the mesoporosity nature of the materials. On the other hand, in the aerobic oxidation of alcohols, the walnut-shell-templated mesoporous magnesia as catalyst support presented considerable activity, which suggests great potential uses in oxidative catalytic processes. The resulting Pd-loaded material acts as an effective catalytic system for the oxidation of a wide variety of alcohols in toluene. The catalyst can be recovered and reused without loss of activity.

Acknowledgment: The authors gratefully acknowledge the financial support for this work by the research council of Urmia University.

References

[1] Adachi S. *Optical Constants of Crystalline and Amorphous Semiconductors*, Springer: Boston, 1999.
[2] Seeger M, Otto W, Flick W, Bickelhaupt F, Akkerman OS. *Magnesium compounds. Ullmann's Encyclopedia of Industrial Chemistry*, Wiley-VCH: Weinheim, 2005, Vol. 22, p 41.
[3] Shand MA. *The Chemistry and Technology of Magnesia*, John Wiley & Sons: New Jersey, 2006.
[4] Yu JC, Xu A, Zhang L, Song R, Wu L. *J. Phys. Chem. B* 2004, 108, 64–70.
[5] Ding Y, Zhang G, Wu H, Hai B, Wang L, Qian Y. *Chem. Mater.* 2001, 13, 435–440.
[6] Hanif A, Dasgupta S, Nanoti A. *Ind. Eng. Chem. Res.* 2016, 55, 8070–8078.
[7] Cao C-Y, Qu J, Wei F, Liu H, Song W-G. *ACS Appl. Mater. Interfaces* 2012, 4, 4283–4287.
[8] Liu Y, Li Q, Gao S, Shang JK. *J. Am. Ceram. Soc.* 2011, 94, 217–223.
[9] Zhang L, Fu W, Xiang M, Wang W, He M, Tang T. *Ind. Eng. Chem. Res.* 2015, 54, 5580–5588.
[10] Tian P, Han X, Ning G, Fang H, Ye J, Gong W, Lin Y. *ACS Appl. Mater. Interfaces* 2013, 5, 12411–12418.
[11] Vu A-T, Jiang S, Kim Y-H, Lee C-H. *Ind. Eng. Chem. Res.* 2014, 53, 13228–13235.
[12] Klabunde KJ, Stark J, Koper O, Mohs C, Park DG, Decker S, Jiang Y, Lagadic I, Zhang D. *J. Phys. Chem.* 1996, 100, 12142–12153.

[13] Baumann SO, Schneider J, Sternig A, Thomele D, Stankic S, Berger T, Grönbeck H, Diwald O. *Langmuir*. 2015, 31, 2770–2776.

[14] Li W-C, Lu A-H, Weidenthaler C, Schüth F. *Chem. Mater*. 2004, 16, 5676–5681.

[15] Purwajanti S, Zhang H, Huang X, Song H, Yang Y, Zhang J, Niu Y, Meka AK, Noonan O, Yu C. *ACS Appl. Mater. Interfaces* 2016, 8, 25306–25312.

[16] Li H, Zhang L, Dai H, He H. *Inorg. Chem.* 2009, 48, 4421–4434.

[17] Zhou J, Wang W, Cheng Y, Zhang Z. *Integr. Ferroelectr.* 2012, 137, 18–29.

[18] Yang S, Huang P, Peng L, Cao C, Zhu Y-N, Wei F, Sun Y, Song W. *J. Mater. Chem. A* 2016, 4, 400–406.

[19] Nelson WM. *ACS Symposium Series* 2004, 887, 7–21

[20] Chheda JN, Huber GW, Dumesic JA. *Angew. Chem. Int. Ed.* 2007, 46, 7164–7183.

[21] Höfer R, Bigorr J. *Green Chem. Lett. Rev.* 2008, 1, 79–97.

[22] Zhou C-H, Xia X, Lin C-X, Tong D-S, Beltramini J. *Chem. Soc. Rev.* 2011, 40, 5588–5617.

[23] Rouquerol F, Rouquerol J, Sing K. *Adsorption by Powders and Porous Solids*, Academic Press: San Diego, 1999, pp 18–20.

[24] Pillai UR, Sahle-Demessie E. *Green Chem.* 2004, 6, 161–165.

[25] Layek K, Maheswaran H, Arundhathi R, Kantam ML, Bhargava SK. *Adv. Synth. Catal.* 2011, 353, 606–616.